Utilizing Building-level Demand Response in Frequency Regulation of Actual Microgrids

Dawei He, Jie Mei, Ronald Harley, and Thomas Habeter
School of Electrical and Computer Engineering
Georgia Institute of Technology
Atlanta, USA
hedawei.david@gmail.com

***Abstract*—This paper presents a methods of utilizing building-level demand response in microgrid frequency regulation. Based on an in-depth study of building loads, a bi-level framework of building demand response control is presented to determine the controllability and demand response participation timescale of different loads. Based on this framework, the internal control scheme of buildings is presented in analogy to negative generators. The contribution of building-level demand response to microgrid frequency regulation is discussed in details. The large power loss on transmission lines in microgrids is considered, and the heterogeneity among buildings in their contribution to system frequency deviation is discussed. A test case is studied to prove the efficacy of building-level demand response in microgrid frequency regulation, and the advantage of building-level demand response over single-load demand response.**

***Index Terms*— demand response, microgrid, frequency regulation, load study, bi-level framework, distribution system power flow**

I. INTRODUCTION

In recent years, the value of demand response (DR) has been detected in-depth by a variety of scholars. A large-scale incorporation of demand response is able to not only reduce the energy bills of consumers [1], but also ease power system operation by means of peak load reduction [2], load following [3] and reserve provision [4]. Many demonstration projects have been conducted to study impact of consumer-level demand response. Results of PNNL's demonstration projects show that a successful building demand response management can effectively reduce the peak energy consumption by 15-20% [5].

Meanwhile, microgrid has come up as an important solution to large-scale penetration of renewable energy, namely wind and photovoltaic (PV). By 2010, the world market for microgrid had reached over $4 billion, and it is expected to continue growing with the spurred growth of renewable energy [6]. However, because of the fluctuating nature of renewable energy, frequency regulation has been an important challenge of microgrid control and operation. Traditional practice tends to equip microgrids with storage devices and sufficient spinning reserve, but it has proved to be costly and economically inefficient.

Demand response, in this case, is a good solution to microgrid frequency regulation. However, there are mainly two bottlenecks for its actual application in microgrid frequency regulation. First, few works on demand response discuss its contribution to system frequency regulation, yet most of them only consider frequency regulation at the transmission level [4][7-9]. Second, in terms of control approaches, almost all previous works from scholars take a direct load control (DLC) approach on selected demand responsive loads, e.g. HVACs, PHEVs and electric water heaters (EWHs) [10][11]. Although effective in small-scale control of several buildings, direct load control is poor in scalability because of the huge number of appliances to be controlled even at the distribution system level [20]. Also, since most of the times only one type of demand responsive loads are utilized, the demand response potential in buildings is not fully exploited.

To deal with these bottlenecks, this paper further develops the authors' idea in [12], and proposes a practical building-level demand response based on a thorough investigation of building loads. This simplifies the distribution level demand response control by controlling buildings as a whole like generators, and buildings can conduct frequency regulation in the same way as AGCs in microgrid or distribution systems.

The rest of this paper is organized as follows. Section II presents the basic scheme of building-level demand response based on a thorough load study. Section III discusses the contribution of buildings to microgrid frequency regulation. Section IV presents a case study to verify the efficacy of building-level demand response and frequency regulation. Section V concludes the paper and presents the authors' future work.

II. BUILDING LEVEL DEMAND RESPONSE BASED ON A THOROUGH LOAD STUDY

Buildings possess a high energy saving potential because of their large share in the total electricity consumption of the US and the huge variety of demand responsive loads in buildings [13]. However, no previous work formally discusses the demand response participation pattern of the diverse loads in a building. Based on [12], this section enumerates the main sorts of demand response participation patterns of building loads, and develops the internal control scheme of building-level demand response.

978-1-4799-0224-8/13/$31.00

A. Bi-level Framework of Building Demand Response Based on Load Investigation

According to the authors' work in [12], there are typically two ways of demand response participation of loads, as is shown in Fig. 1. Level I loads are the main demand responsive loads, which are typically high-power controllable appliances like HVACs, EWHs, space heaters, etc. Level II loads are the back-up demand responsive loads, which are supposed to participate in demand response during critical system operations, like TV and home theaters. Some other critical loads, like fire alarms or modems, are prohibited from demand response because of their vital functions. This classification exploits all the potential demand response resources in a building, and possibly benefits both consumers and the grid, since consumers earn extra fees from offering demand response service and the stability of the power grid is improved at the same time.

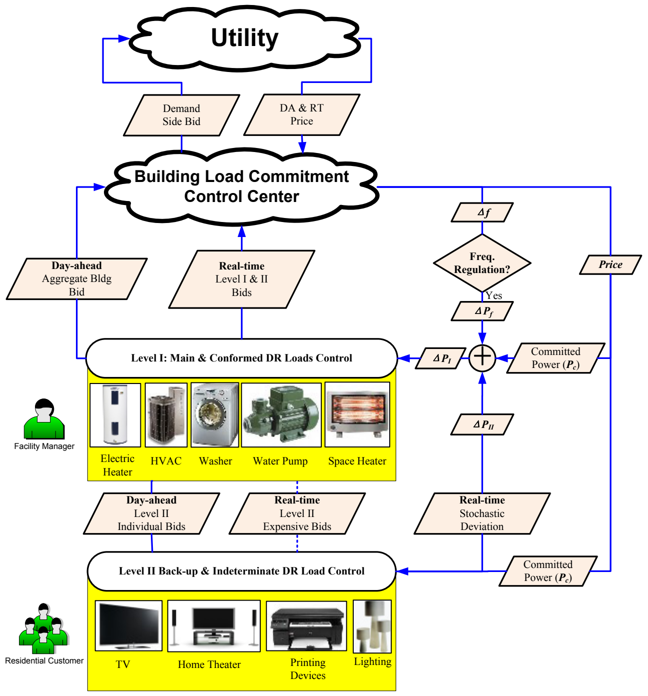

Fig. 1. Bi-Level Framework of Load Participation in Demand Response [12]

In utility level operation, similar to generators, buildings submit their bids in both day-ahead and real-time markets. Based on the price information from the utility, the local building commitment is determined at the building load commitment control center, and the internal controllers in the building mainly manipulates Level I appliances in real time so as to consume the committed amount of electricity. However, if Level I loads are unable to fulfill the control objectives, Level II real-time control can be triggered and the back-up demand responsive loads will be manipulated.

B. Modeling of Selected Loads

In order to control the appliances effectively in demand response, it is necessary to model the steady state and the dynamics of the demand responsive loads. Target loads include HVACs, EWHs, PHEVs, dimmable lights, and the back-up demand responsive loads.

1) HVACs

HVACs are high-power continuously controllable appliances, controlled by temperature set-points. Unlike the differential equation based approaches [14] or other state variable based complex models [15], this paper derives a time-domain HVAC model based on EnergyPlus simulation, and applies it to real-time control cases.

In the steady state, the cooling power of HVAC varies linearly with the temperature set-point, as is shown in equation(1). Here $Q_0(t)$ refers to the baseline thermal load, $T_a(t)$ the ambient temperature, and $\varepsilon(t)$ the stochastic variation item.

$$P(t) = Q(t) = Q_0(t) + k(T_a(t) - T(t)) + \varepsilon(t) \tag{1}$$

During the thermal dynamics, to shorten the duration of the transitional period, HVACs usually ramp up to their max/min power the moment the temperature set-point changes. Then, the temperature varies exponentially until the desired set-point is reached, as shown in equation (2).

$$T = T' - (T' - T_0)e^{t/\tau}, T' - T_0 \overset{\Delta}{=} k \tag{2}$$

The thermal dynamics of HVACs usually lasts for 5-10 min for a 1°C change in temperature set-point. Therefore, the power variation of HVACs differs at different timescales, as is shown in (3)(4). In a short timescale, the power variation is the difference between the original HVAC power and max/min HVAC power. However, at the hourly timescale, the power variation is determined by (1).

$$\Delta P_{HVAC,up} = \begin{cases} P_{rated} - P(t) \; (short\ timescale) \\ k\Delta T \; (long\ timescale) \end{cases} \tag{3}$$

$$\Delta P_{HVAC,down} = \begin{cases} -P(t) \; (short\ timescale) \\ -k\Delta T \; (long\ timescale) \end{cases} \tag{4}$$

2) EWHs

A 2-node model of EWH is developed here, improving that from PNNL in [3][10]. Two state variables are utilized to depict the temperature in an EWH: the top and bottom node temperature. Approximately, the average temperature in the tank is the average of top and bottom temperature.

In demand response control, the determination of the upper/lower limit, as well as the ramp rate of appliances is crucial. EWHs are subject to comfort constraint (5), so when an increase in aggregate EWH power consumption is required, equation (6) gives the maximum possible power increase. An intuitive explanation of equation (6) is that in order to increase the power of EWHs for a time interval of $T_{duration}$, EWHs can heat the water until the water temperature is about to exceed the permitted threshold.

$$\left| T_{top} - T_{set} \right| < \Delta T \tag{5}$$

$$\Delta P_{up,\max} = N(p_{loss} + \frac{cm\Delta T}{T_{duration}}) \tag{6}$$

The only possible approach to decrease EWH power consumption is to delay the heating of EWHs. For EWHs, the power of hot water consumption (p_{hw}) is often greater than the rated heating power (p_{rated}), and heaters are mandated to be on. When hot water consumption stops, heating can be stopped temporarily to decrease the aggregate EWH power. Based on this method, the possible maximum decrease in aggregate EWH power can be given by equation (7). p_{rated}/p_{hw} shows the ratio of hot water consumption duration over heating duration, and N_{use} is the number of EWH users in a given timescale, e.g. an hour. The power of hot water consumption can be calculated by (8), where Q is the hot water flow rate, and T_{top} and T_{in} refer to the temperature of the top node and inlet cold water.

$$\Delta P_{down,\max} = N_{use}[p_{loss} + p_{rated} * (1 - p_{rated} / p_{hw})] \tag{7}$$

$$p_{hw} = cQ\rho(T_{top} - T_{in}) \tag{8}$$

3) PHEVs

Currently, most of the commercial EV chargers follow the SAE J1772 standard [16]. PHEVs can be charged at a fixed power (1.9kW), thus they are considered as high-power ON/OFF control loads. They are subject to charging constraint (9), in which *u(t)* is the on/off status of each hour.

$$\sum_{t=t_{start}}^{t_{end}} P_{rated} u(t) = Q \tag{9}$$

4) Dimmable Lights

The power of dimmable lights can be adjusted instantaneously without ramp rate limit, but they are subject to a comfort constraint, i.e. there is a min requirement on lighting power. The best lighting power is considered to be the rated power, and a quadratic function (10) describes the discomfort level.

$$discomfort(P) = \beta(P - P_{rated})^2 \tag{10}$$

5) Back-up Demand Responsive Loads

There are three types of usage behaviors of back-up demand responsive loads, as is shown in Table I. For the violation behavior, a penalty will be mandated. For the determinate behavior, there can be an emergent load shedding during extreme frequency deviation. For the stochastic loads, their power consumption can be modeled by Markov Chain in equation (11).

$$P_{sto}(t + \Delta t) = P_{sto}(t) + \varepsilon(t, \Delta t),\ \varepsilon(t, \Delta t) \sim \quad \Delta t) \tag{11}$$

TABLE I
DEFINITION OF BACK-UP DEMAND RESPONSIVE LOAD USAGE BEHAVIOR

Day-head Scheduling	**Deviation from Scheduling**	**Usage Behavior**
Y	Y	Violation
Y	N	Determinate
N	N/A	Stochastic

C. *Block Diagram of Building Internal Control*

Previous works like [8][11][17] have demonstrated that buildings can be controlled to deliver a desired level of power consumption. Therefore, in controlling buildings as a whole, it is possible to consider them as a negative generator, and they possess internal control schemes similar to AGC.

Based on the bi-level framework presented in part A, a block diagram of building internal control is developed in Fig. 2. Most of the times, Level I loads serve as the controllable loads of the building, yet under critical system conditions (over/under frequency), Level II loads can participate in frequency regulation. In this control scheme, the desired change in Level I appliance power (ΔP_I) is first calculated, and then allocated to different appliances based on their power variation potential. Then local controllers manipulate individual loads to reach to desired power change. Subject to the ramp rate constraint and upper/lower power limit, the eventual change in Level I power is determined. Then the actual change in system power imbalance is obtained by adding together the change in building power ($\Delta P_I + \Delta P_{II}$), and stochastic external disturbance (ΔP_D). An inertia block is used to determine frequency deviation, in which the system inertia is depicted by M and the ratio of p.u. power change over p.u. frequency change is D. All these abovementioned control steps constitute the internal control scheme of buildings in demand response.

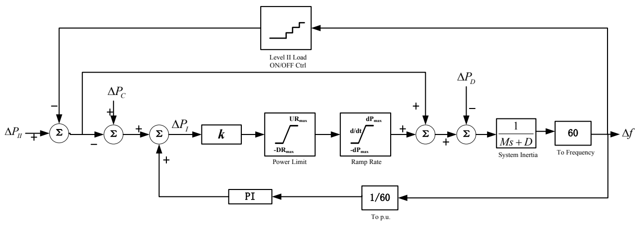

Fig. 2 Block Diagram of Building Internal Control

III. ANALYSIS OF THE CONTRIBUTION OF BUILDING TO MICROGRID FREQUENCY REGULATION

A. *Role of Buildings in Microgrid Frequency Regulation*

The role of demand responsive buildings in microgrid frequency regulation can be divided into two parts. First, in normal operation cases, which can be well-handled by traditional AGC units of the microgrid, building-level demand response assists in microgrid frequency regulation to alleviate frequency deviation. Second, during critical hours of system operation, building demand response performs excessive frequency regulation, so as to prevent the microgrid from collapse without bringing significant consumer discomfort.

B. *Determination of Building ACE Signal Based on Microgrid Power Flow Characteristics*

Consider a microgrid with traditional generation units, e.g. diesel generators or gas turbines. The frequency deviation of the microgrid actually results from the difference between the mechanical power input and the electrical power output of these units, as is illustrated in equation (12).

$$\Delta\omega(t) = \frac{1}{2H}\int_0^t (T_m(t) - T_e(t))dt = \frac{1}{2H}\int_0^t \frac{P_m(t) - P_e(t)}{\omega(t)}dt \quad (12)$$

While $P_m(t)$ is normally regulated by AGC, $P_e(t)$ can be controlled by building-level demand response. With enough real-time data of the active and reactive power consumption of every individual building, the power flow at each line connected to the generators can be calculated, and P_e can be obtained by the power flow equation.

$$P_e = \sum_{i\in G}\sum_{j=1}^{N} P_{ij} = f(\mathbf{P}_{bldg}, \mathbf{P}_{renewable}) \quad (13)$$

Here G refers to the set of nodes connected to generators. Let λ_i denote the sensitivity of P_e to the power of the i^{th} building, then ΔP_e can be expressed in a linear way.

$$\Delta P_e = \sum_{i=1}^{M_1} \lambda_i \Delta P_{bldg,i} + \sum_{j=1}^{M_2} \lambda_j \Delta P_{renewable,i} \quad (14)$$

λ_i can be referred to as the contribution factor of the i^{th} building, and it can be calculated numerically, given the day-ahead committed power of buildings at each hour. If the i^{th} building possesses a relatively large value of λ_i, it means that it is able to make a greater contribution to system frequency regulation. Hence, to capitalize the more 'crucial' buildings in frequency regulation, the ACE signal for the i^{th} building can be given by the equation below.

$$ACE_i = \lambda_i k \bullet \quad (15)$$

Where k is a constant determining the amount of system ACE that are to be handled by buildings.

IV. Simulation Case Study

A. Simulation Setup

An island microgrid test case adopted from [18][19] is presented in Fig. 3 and Table II. Assume that V_N = 10kV and S_N=10MVA, the capacity of diesel generator is 10MW, and that of wind turbine is 3MW. Data of wind generation are selected from NREL EWITS database. The max energy consumption in each building is 2.5MW. There are 4 sorts of Level I loads in the demand responsive buildings: HVACs, EWHs, PHEVs and dimmable lights. The allocation coefficient ***k*** is determined in proportion to the maximum capacity of the loads, as is shown in Table III. The control parameters of the demand responsive loads and the diesel generator is presented in Table IV, and the comfort constraint of HVACs is shown in Table V.

Two simulation scenarios are discussed. First, a daily frequency variation of the microgrid with and without building-level demand response is presented, and the demand response potential is compared between building-level and single-load demand response. Second, a collapse in wind generation is assumed, and the microgrid frequency deviation during critical hours is considered.

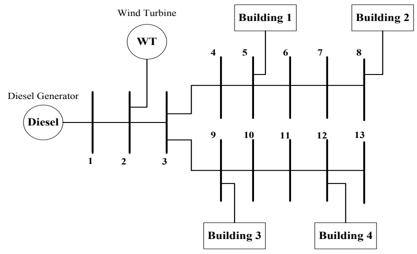

Fig. 3 Island Microgrid Test Case

TABLE II
TEST SYSTEM LINE IMPEDENCES

Lines	Impedance (p.u.)
Node1-2, 2-3	0.0475+j0.2018
Between Other 2 Nodes	0.02+j0.02

TABLE III
CONTROL PARAMETERS IN PER UNIT VALUE

Load/Generator	P_{max}	P_{min}	Ramp Rate (sec)	*k* Coefficient
HVAC	1	0	0.5	0.4
EWH	1	0	1	0.2
PHEV	1	0	1	0.35
Lighting	1	0	0.1	0.05
Diesel	1	0.1	1/1200	-

TABLE IV
COMFORT CONSTRAINT OF HVACS

Parameter	T_{set}	ΔT	τ	Q_0	k
Value (p.u.)	24°C	±2°C	10min	0.01	0.1

B. Simulation Results

First of all, daily variation of wind power is presented in Fig. 4, and variation of contribution factor is presented in Fig. 5. The contribution factors are time-variant because of the variant operation points of the microgrid.

Next, the comparison between building-level and single-load demand response is presented in Fig. 6 and 7. Apart from exploiting more loads into demand response, building-level demand response has the advantage of a smoother demand response potential during the whole day, which is more desirable for microgrid operation.

Fig. 8 presents the microgrid frequency deviation with and without demand response, and Fig. 9 presents the corresponding variation of building internal temperature. These two figures show that building-level demand response is able to stabilize microgrid frequency without violating the comfort constraint. Additionally, the consideration of difference in distribution factors decreases standard deviation of Δf from 0.0035Hz to 0.0031Hz.

Last but not least, the impact of demand response on frequency regulation during critical hours is presented in Fig. 10. In this figure, an imaginary collapse of wind generation occurs from 19:00 to 20:00, and the pick-up of wind generation then lasts from 20:00 to 22:00. It can be found that demand response effectively reduces the maximum frequency drop and the duration of system frequency oscillation.

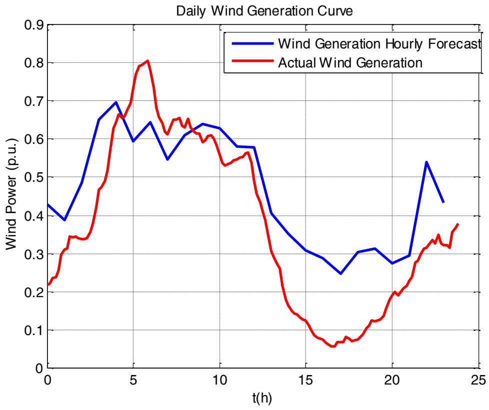

Fig. 4 Daily Variation of Wind Turbine Generation

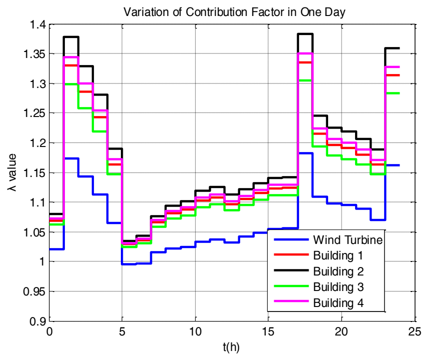

Fig. 5 Variation of Contribution Factor of Wind Turbine and Buildings

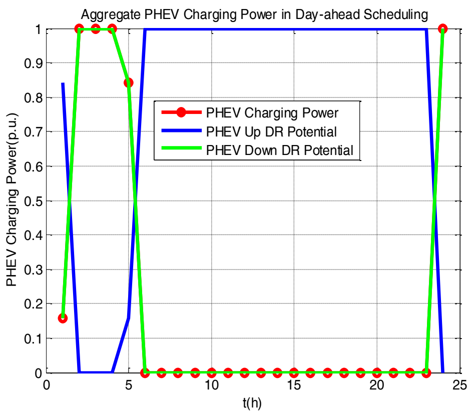

(a)

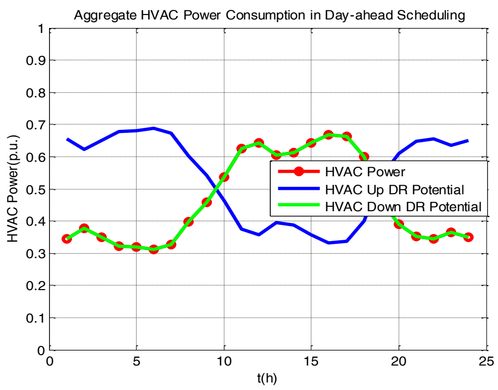

(b)

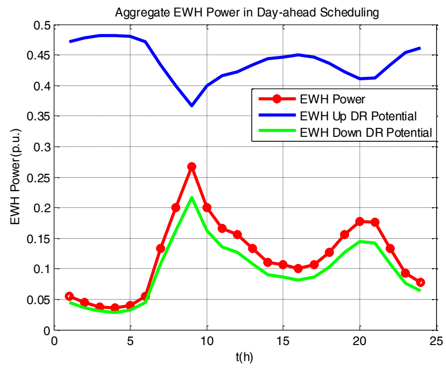

(c)

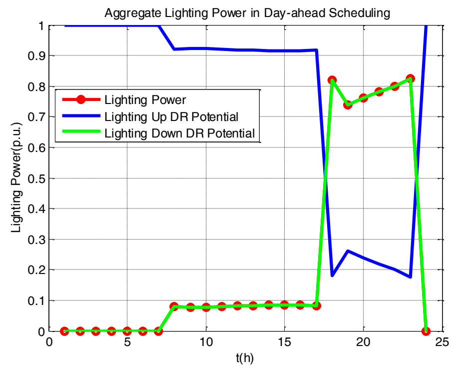

(d)

Fig. 6 Single Appliance Demand Response Potential in p.u. : (a) PHEV; (b) HVAC; (c) EWH; (d) Dimmable Lighting

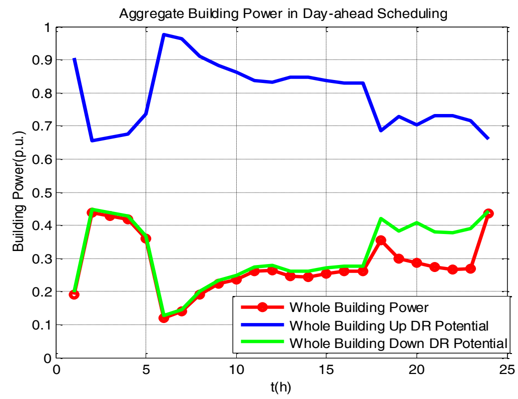

Fig. 7 Aggregate Building Demand Response Potential in p.u.

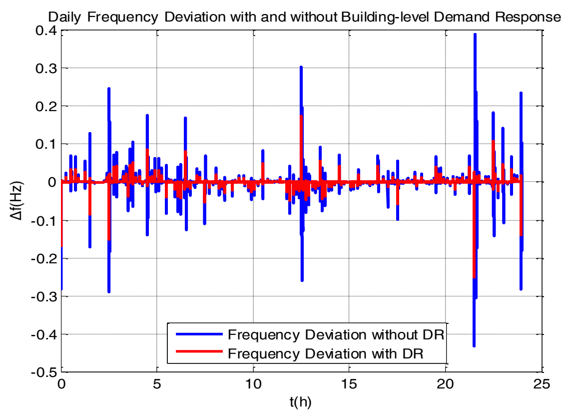

Fig. 8 Frequency Deviation in 24h with and without Demand Response

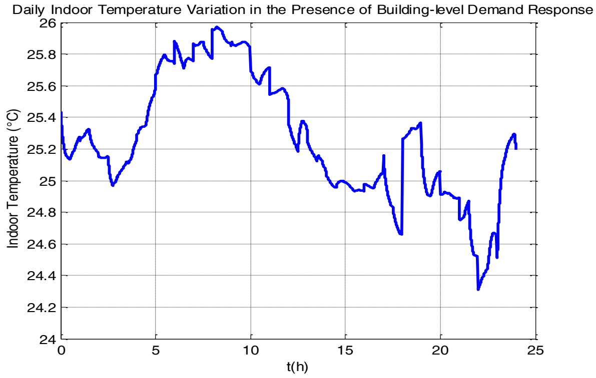

Fig. 9 Variation of Bldg Temperature in the Presence of Demand Response

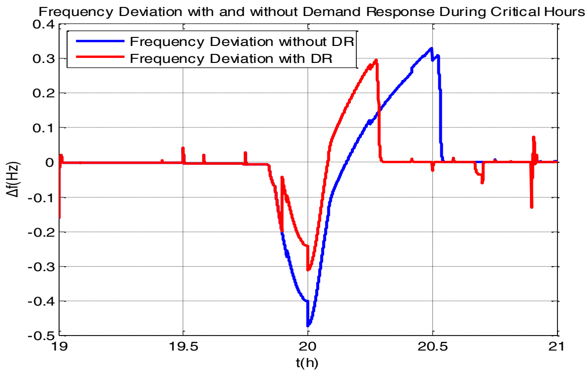

Fig. 10 Frequency Deviation with and without Demand Response during Critical Hours of the Day

V. CONCLUSION AND FUTURE WORK

This paper presents a building-level demand response control scheme based on a thorough load study, and applies it to microgrid frequency regulation. The findings of this paper can be summarized as follows.

First, compared with single-load demand response, building-level demand response is able to provide a more smooth demand response potential during the whole day, and is able to exploit more demand responsive loads in buildings.

Second, in microgrid frequency regulation, during normal operation scenarios, building-level demand response alleviates the frequency deviation, while in extreme scenarios it is able to improve the dynamic frequency characteristics of the microgrid considerably. The consideration of different distribution factors amongst buildings is also proved to be effective.

In the future, the authors are planning to study the problem further in two aspects. On one hand, the contribution of building-level demand response in microgrid voltage control, stability and reliability will be studied. On the other hand, further study about proper control algorithms of building internal and external control will all be considered.

REFERENCES

[1] N. Zhang, *et al.*, "Investigating the Impact of Demand Side Management on Residential Customers", in *Innovative Smart Grid Technologies (ISGT Europe), 2011 2nd IEEE PES International Conference and Exhibition on*, Dec 2011.

[2] A. Mohsenian-Rad, *et al.*, "Autonomous Demand-Side Management Based on Game Theoretic Energy Consumption Scheduling for the Future Smart Grid", *Smart Grid, IEEE Transactions on*, vol. 1, no. 3, pp. 320-331, Dec. 2010.

[3] J. Kondoh, *et al.*, "An Evaluation of the Water Heater Load Potential for Providing Regulation Service," *Power Systems, IEEE Transactions on*, vol. 26, no. 3, pp. 1309–1316, Aug. 2011.

[4] K. Schisler, *et al.*, "The Role of Demand Response in Ancillary Service Markets", in *IEEE/PES Transmission and Distribution Conference and Exposition (T&D) 2008*, April 2008.

[5] D. J. Hammerstrom, *et al.*, Pacific Northwest GridWise Testbed Projects: Part 1. Olympic Peninsula Project, PNNL-17167, Pacific Northwest National Laboratory. Richland, WA, 2007.

[6] SBI Energy, "The World Market for Microgrids," Online report, Feb 1, 2011, http://www.sbireports.com/Microgrids-2835891/, July 2011.

[7] A. Molina-García, *et al.*, "Decentralized demand-side contribution to primary frequency control," *Power Systems, IEEE Transactions on,* vol. 26, no. 1, pp. 411–419, 2011.

[8] L. Jia, *et al.*, " Multi-Scale Stochastic Optimization for Home Energy Management," in *Computational Advances in Multi-Sensor Adaptive Processing (CAMSAP), 2011 4th IEEE International Workshop on*, pp. 113-116, 2011.

[9] S. A. Pourmousavi and M. H. Nehrir, "Real-time Central Demand Response for Primary Frequency Regulation in Microgrids", *Smart Grid, IEEE Transactions on*, accepted for future inclusion.

[10] P. Du and N. Lu, "Appliance Commitment for Household Load Scheduling," *Smart Grid, IEEE Transactions on,* vol. 2, no. 2, pp. 411-419, Jun. 2011.

[11] D. S. Callaway, "Tapping the Energy Storage Potential in Electric Loads to Deliver Load Following and Regulation, with Application to Wind Energy," *Energy Conversion and Management*, vol. 50, no.9, pp. 1389-1400, 2009.

[12] D. He, *et al.*, "Incorporating the Non-intrusive Load Monitoring Technology into Demand Response", *Smart Grid, IEEE Transactions on*, accepted.

[13] D. He *et al.*, "Front-End Electronic Circuit Topology Analysis for Model-Driven Classification and Monitoring of Appliance Loads in Smart Buildings," *Smart Grid, IEEE Transactions on,* accepted for future inclusion.

[14] J. Rehrl and M. Horn, "Temperature Control for HVAC Systems based on Exact Linearization and Model Predictive Control", in *Control Applications (CCA), 2011 IEEE International Conference on*, Sept 2011.

[15] N. Lu, "An Evaluation of the HVAC Load Potential for Providing Load Balancing Service," *Smart Grid, IEEE Transactions on*, vol. 3, no. 3, pp. 1263-1270, Sept. 2012.

[16] SAE Electric Vehicle and Plug in Hybrid Electric Vehicle Conductive Charger Coupler. Available Online: http://standards.sae.org/j1772_201210/

[17] Z. Zhou *et al.*, "Agent-Based Electricity Market Simulation With Demand Response From Commercial Buildings," *Smart Grid, IEEE Transactions on* , vol.2, no.4, pp.580-588, Dec. 2011.

[18] T. Senjyu, *et al.*, "Optimal Distribution Voltage Control and Coordination with Distributed Generation", *Power Delivery, IEEE Transactions on*, vol. 23, no. 2, pp. 1236-1242, April 2008.

[19] M. Tokudome, *et al.*, "Frequency and Voltage Control of Isolated Island Power Systems by Decentralized Controllable Loads", in *Transmission and Distribution Conference and Exposition: Asia and Pacific 2009*, Oct 2009.